



Characterization of Brazilian in-home power line channels for data communication



Thiago R. Oliveira^{a,*}, Antonio A.M. Picorone^b, Sergio L. Netto^c, Moises V. Ribeiro^d

^a Electronics Department, Federal Institute of Education, Science and Technology of the Southeast of Minas Gerais (IFSEMG), Campus Juiz de Fora, Brazil

^b Electrical Engineering Department, Federal University of Juiz de Fora (UFJF), Brazil

^c Electrical Engineering Program at COPPE-Federal University of Rio de Janeiro (UFRJ), Brazil

^d Electrical Engineering Department, Federal University of Juiz de Fora (UFJF), and Smarti9 Ltda, Brazil

ARTICLE INFO

Article history:

Received 1 February 2017

Received in revised form 23 April 2017

Accepted 9 May 2017

Keywords:

Channel characterization
Power line communication
Coherence time
Data rate
Access impedance

ABSTRACT

This paper focuses on the characterization of Brazilian in-home power line channels for data communication when a sounding-based approach is applied. Based on a measurement campaign carried out in seven Brazilian residences, a statistical characterization of frequency response magnitude, average channel gain, coherence bandwidth, root mean squared delay spread, coherence time, achievable data rate, additive noise and access impedance are presented, considering the frequency bands from 1.7 up to 30, 50 and 100 MHz. Comparative analysis considering previous contributions show disparities and similarities among typical in-home power line channels measured in different countries. The attained results reveal that average channel gain in Brazil is higher than in other countries, the linear relationship between average channel gain and root mean squared delay spread and the inverse relation between coherence bandwidth and root mean squared delay spread are confirmed. Moreover, these results show that coherence bandwidth in Brazil is wider than in European countries, root mean squared delay spread in Brazil is shorter than in US and European countries and coherence time in Brazil is shorter than what is previously reported in the literature.

© 2017 Elsevier B.V. All rights reserved.

1. Introduction

There is a growing interest in the use of electric power grids for data communications purposes. In fact, power line communication (PLC) systems and their applications have been investigated by academic and business sectors. As electric power grids were not originally designed for data communication purposes, they constitute a challenging medium, in which the transmitted signals suffer severe attenuation and are strongly corrupted by colored and impulsive noise. Also, the diversity of topologies of electric power grids and the dynamic of the connected devices (loads) make these grids hard to characterize and model.

In this sense, an expressive effort for the characterization of PLC channels is needed in order to allow a better exploitation of such challenging and opportunistic data communication medium. Indeed, there are some contributions in the literature about this

issue and they can be classified according to the voltage level and frequency bandwidth. For instance, the outdoor PLC channel can be evaluated for low-voltage [1], medium-voltage [2,3] and high-voltage [4]. Also, underground medium-voltage PLC channels are evaluated in [5] while [6] deals with overhead conductors. For the indoor-PLC channel case, there is the following subdivision: residential or commercial buildings (usually referenced as in-home) [7,6], and in-vehicles (cars [8], ships [9] and aircrafts [10]). Finally, the PLC channel characterization can be performed by considering distinct bandwidths, usually classified as narrowband and broadband. The narrowband PLC comprises the frequencies up to a few hundreds kHz and are used for low data rate applications [11,12]. On the other hand, for broadband PLC systems the investigated bandwidths are those limited to the frequency of 30 MHz [13], which is regulated in some European countries, and to the frequency of 100 MHz [7], in which data rate in the order of 1–2 Gbps can be achieved. In Brazil, the telecommunication regulatory authority allows that broadband PLC systems operate in the frequency band from 1.7 up to 50 MHz which is a frequency band that lacks characterization. There are also few works that provide analysis covering the frequency band of up to 300 MHz [14,15].

* Corresponding author.

E-mail addresses: thiago.oliveira@ifsudestemg.edu.br (T.R. Oliveira), picorone@ieee.org (A.A.M. Picorone), sergioln@smt.ufrj.br (S.L. Netto), mribeiro@ieee.org (M.V. Ribeiro).

Focusing on the in-home PLC scenario, some few contributions related to developed countries can be highlighted. For PLC channels in Spain, [16] presented results of channel attenuation and noise, for frequencies up to 30 MHz, while [17] considered other features, such as the average channel gain (ACG), the delay spread and the coherence bandwidth (CB). Also, [18] discussed the normality/lognormality natures of the ACG and delay spread. More recently, [14] analyzed the ACG, CB and root mean squared delay spread (RMS-DS) considering the frequency band from 1.8 up to 100 MHz and also expanding the upper frequency edge to 300 MHz. In [19,13], the in-home PLC channels in some urban and suburban United States (US) residences were characterized in terms of ACG and RMS-DS, considering the frequency band ranging from 2 up to 30 MHz. The results reported for in-home PLC channels in France are found in [7,20], where the PLC channel is evaluated in terms of ACG, CB and RMS-DS, for frequencies up to 100 MHz. The analysis related to the time varying behavior of PLC channel was addressed in some few works, such as [21,22], and lacks a more thorough statistical analysis. Furthermore, there are few works that address the analysis of access impedance [14,23].

This work aims to offer the first characterization of in-home PLC channels in Brazil, constituting an important reference to support future efforts in modeling and designing in-home broadband PLC systems. Preliminary results were reported in [24], in which the average channel attenuation (ACA), the RMS-DS and the achievable data rate were briefly discussed from a small set of measured Brazilian in-home PLC channels, considering the frequency band ranging from 1.7 up to 30 MHz. In this contribution, three distinct frequency bands, 1.7 up to 30 MHz (Band A), 1.7 up to 50 MHz (Band B) and 1.7 up to 100 MHz (Band C), are considered. The Band A agrees with telecommunication regulation over PLC systems imposed by some European countries [13], Band B comprises the regulation for Brazilian telecommunication regulatory authority to PLC systems [25], and Band C represents a tendency for future PLC systems since data rate in the order of 1–2 Gbps can be achieved [26]. In this regard, a measurement campaign was performed in seven middle class places in an urban area, totalizing 245 different channel configurations (only 27 channel configurations were taken into account in [24]), for which the following features were estimated and statistically characterized:

- Channel frequency response (CFR): It allows quantify the attenuation introduced by the PLC channel in each frequency.
- Average channel attenuation (ACA): It is the mean attenuation introduced by a PLC channel.
- Root mean squared delay spread (RMS-DS): It is related to the channel dispersion due to multipath phenomena.
- Coherence bandwidth (CB): It reflects how flat the channel frequency response is.
- Coherence time (CT): Period of time in with the PLC channel can be considered time invariant.
- Power spectrum density (PSD) of the additive noise: Gives the power distribution of the noise in respect to the frequency.
- Achievable data rate: It is the maximum data rate that can be transmitted through the PLC channel.
- Access impedance: Impedance at the power line access point.

Also a discussion about temporal variation of some channel parameters and their correlation with the mains signal are presented. Finally, the results are compared to those discussed in the literature for in-home PLC channel in other countries.

The remainder of this work is organized as follows: Section 2 presents the complete setup used for the PLC channel characterization, Section 3 describes the performed measurement campaign, whereas Section 4 briefly presents the computation method applied to estimate the desired PLC channel features. In

Section 5, the results are presented and discussed, while the work conclusions are summarized in Section 6.

2. Measurement setup

The characterization of the measured Brazilian in-home PLC channels was supported, for the most part, by estimates of the CFR. Complementary characterization were performed though measurements of the noise PSD. A CFR measurement setup illustration is depicted in Fig. 1. As we can see, the setup consists of three main components:

- Signal generator: It is an equipment composed of an arbitrary signal generator board mounted in a rugged computer. A pre-designed sounding sequence is loaded into it and converted to an analog signal to be injected into the PLC channel under analysis. The signal generator has 12 bits of resolution, can generate signal in the range of ± 870 mV and its data sheet can be accessed in [27].
- Data digitizer: It acts as a receiver, acquiring the transmitted sounding signal after its propagation through the PLC channel, and converts it into a digital representation for the subsequent analysis. The adopted acquisition board has 16 bits for quantization. It was set to operate with a resolution of, approximately, $30.5 \mu\text{V}$ and has an embedded anti-aliasing filter. Some additional technical information can be accessed in [28].
- Coupler: Circuitry used to connect both the signal generator and the data digitizer to the PLC channel under analysis. The coupler is essentially a capacitive passband filter [29], blocking the main voltage signal (60 Hz in Brazil) that can damage the equipment (signal generator and data digitizer) and avoiding aliasing.

The signal used to estimate the CFR of PLC channel under analysis is loaded into the signal generator (transmitter) and converted in an analog signal at the rate of $f_s = 1/T_s = 200$ MHz. This transmitted signal is composed of Hermitian symmetric orthogonal frequency division multiplexing (HS-OFDM) symbols [30] and result in a base-band signal in time domain. Each symbol has $2N = 4096$ binary phase shift keying (BPSK) modulated subcarriers and a cyclic prefix (CP) composed by the last 512 samples appended at the beginning of the symbol. At the data digitizer (receiver), the distorted and corrupted version of the generated signal (due to its propagation through the PLC channels) is stored at a sample rate of $f_s = 200$ MHz.

With the possession of the discrete-time version of both the generated and acquired (extracted) signals, a channel-estimation method is performed. The method encompasses the following functionalities [31]:

- Sampling-frequency offset (SFO) correction: It is necessary because the clock sources in the signal generator and data digitizer are different. The technique applied to correction of SFO used in this work is based on a cubic interpolation [32].
- Input-output timing synchronization: This step is based on the CP redundancy incorporated to the HS-OFDM symbol [33]. The correlation operator is used in order to identify the beginning of each symbol within the data recorded at the receiver.
- Channel estimation: A CFR estimate is obtained using the transmitted and received symbols, both in frequency domain.
- Channel estimation enhancement: This procedure was proposed in [34] and it is used to mitigate the noise effects in the CFR estimates. Assuming that the CIR length is lower than the length of the transmitted signal, thus the last samples of the estimated channel impulse response are just noisy coefficients that can be disregarded (replaced by zero), to attain a more reliable estimate. In this work we assume that the length of the CIR is equal to the length of the CP.

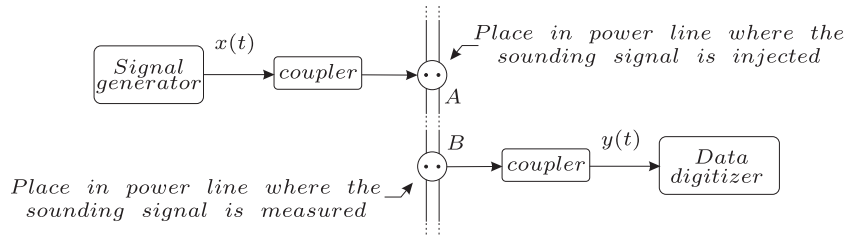


Fig. 1. PLC measurement setup.

Table 1
Main features of the measured places.

Construction type	Age (years)	Constructed area (m ²)	Considered outlets
House # 1	30	78	12
House # 2	10	69	14
Apartment # 1	9	54	11
Apartment # 2	9	42	06
Apartment # 3	18	65	11
Apartment # 4	3	62	11
Apartment # 5	2	54	11

This estimation method results in reliable CFR estimates if the PLC channel is time invariant during a time interval higher than a HS-OFDM symbol time duration. Based on the chosen estimation parameters, an enhanced channel estimate is obtained every $T = (2N + L_{cp})T_s = 23.04 \mu\text{s}$, approximately, where L_{cp} is the length of CP. Furthermore, according to [21], $600 \mu\text{s}$ is the minimum interval of time within which the PLC channel can be considered time invariant. Thus the presented method is suitable for PLC CFR estimation and permits analysis related to temporal variations of channels. Also, by the adopted value of N and the considered frequency bandwidth ($B = 100 \text{ MHz}$), the resulting CFR estimate has a frequency resolution around $\Delta_f = 48.83 \text{ kHz}$.

For the measurement of the noise PSD the data digitizer was used when no sounding signal was being transmitted.

Finally, the access impedance was measured by a vectorial network analyzer that operates in a frequency range beginning in 2 MHz . This equipment was connected to the power line through the coupler described above.

3. Measurement campaign

Seven different middle class residences in Brazilian urban area of Juiz de Fora city were considered. Some features of these places are summarized in Table 1. From the entire campaign, 245 different combinations of pairs of outlets were measured, providing a total of 148,037 different CFR estimates, with an average of 604 consecutive CFR estimates for each PLC channel configuration. Furthermore, the noise in power line and the access impedance were measured in each considered outlet, resulting in a total of 76 distinct noise and access impedance measures.

4. PLC channel features

The well known features that are used for characterizing the in-home PLC channels are described in the following subsections.

4.1. Average channel attenuation

The ACA is expressed by

$$\text{ACA} = -\text{ACG} = -10 \log_{10} \left(\frac{1}{N} \sum_{k=0}^{N-1} |H[k]|^2 \right), \quad (1)$$

where N is the subcarrier number and $H[k]$ is the k th coefficient of the discrete Fourier transform of the channel impulse response, $\{h[n]\}_{n=0}^{N-1}$, of a linear and time invariant PLC channel.

4.2. Root mean squared delay spread

The RMS-DS represents the distribution of the transmitted power over the various paths in a multipath environment. It can be defined as the square root of the second central moment of a power delay profile. For a discrete time channel impulse responses (CIR), the RMS-DS is expressed as

$$\text{RMS-DS} = T_s \sigma_0 = T_s \sqrt{\mu_0' - \mu_0^2}, \quad (2)$$

where

$$\mu_0 = \frac{\sum_{n=0}^{N-1} n |h[n]|^2}{\sum_{n=0}^{N-1} |h[n]|^2}, \quad \mu_0' = \frac{\sum_{n=0}^{N-1} n^2 |h[n]|^2}{\sum_{n=0}^{N-1} |h[n]|^2}, \quad (3)$$

and $T_s = 1/f_s$ is the sampling period. Note that σ_0 is the RMS-DS normalized to unitary sampling time, μ_0 is the average delay, and $h[n] = h(t)|_{t=nT_s}$ is the n th sample of the discrete time CIR.

4.3. Relationship between RMS-DS and ACA

According to [13], the relationship between the RMS-DS and the ACA can be approximated by

$$\text{RMS-DS}(\mu\text{s}) = \alpha \cdot \text{ACA} + \beta. \quad (4)$$

This relationship indicates that PLC channels with high values of RMS-DS exhibit high attenuation.

4.4. Coherence bandwidth

The CB reflects how flat is the channel frequency response. In this contribution, this metric is calculated through a correlation computed of each channel frequency response, and is defined as deterministic CB in [14]. All the results of CB referenced in this work were obtained using it.

First, let the correlation function given by

$$\rho_H(l) = \sum_{k=0}^{N-1} H[k] H^*[(k+l)_N], \quad (5)$$

where $\{*\}$ denotes the complex-conjugate operation. The CB (l_c) is obtained by

$$|\rho_H(l_c)| \geq \varphi, \quad (6)$$

where $\varphi \in \mathbb{R} \quad | \quad \varphi \in [0, 1]$ refers to the lowest correlation level on which it was observed a discrete CB value of l_c . The CB in Hz is given by $\text{CB} = l_c \Delta_f$, in which Δ_f is the frequency resolution. The

correlation levels (φ) of 0.9, 0.7 and 0.5 are considered in this contribution.

4.5. Relationship between CB and RMS-DS

The relationship between the CB and the RMS-DS is generally expressed by

$$\text{RMS-DS} \approx \frac{\gamma}{\text{CB}}, \quad (7)$$

where γ is a constant that depends of the channel type, CB (in kHz) is the coherence bandwidth at a correlation level of 0.9 and RMS-DS is given in microseconds.

4.6. Coherence time

The CT is the time duration in which the CIR can be considered time invariant. The CT can be evaluated as [35]

$$\text{CT}^\beta = M_c T_{\text{sym}}, \quad (8)$$

where M_c is the number of consecutive channel measurements needed to reach a correlation equal to β and T_{sym} is the symbol duration.

4.7. Achievable data rate

Let PLC channel be frequency selective, and the additive noise be colored Gaussian random process, then the achievable data rate can be evaluated as [36]

$$C = \max_{S_x[k]} \frac{B}{N} \sum_{k=0}^{N-1} \log_2 \left(1 + \frac{S_x[k] \cdot |H[k]|^2}{S_N[k]} \right) \quad (\text{bps}), \quad (9)$$

where B is the frequency bandwidth; $S_x[k]$ and $S_N[k]$ denote the k th coefficient of the power spectral densities of the transmitted signal and the additive noise, respectively; $\frac{B}{N} \sum_{k=0}^{N-1} S_x[k] = P_x$, in which P_x is the transmission power and N is the subcarrier number.

5. Numerical analysis

In this work, the in-home PLC channel estimation and characterization were performed by addressing the three distinct frequency bands: (i) Band A (1.7–30 MHz), (ii) Band B (1.7–50 MHz) and (ii) Band C (1.7–100 MHz). The characterization of in-home PLC channels features are presented and discussed in the following subsections.

5.1. Channel magnitude function

By considering Band C, which encompasses Band A and Band B as well, some interesting features of the in-home PLC channel magnitude response are depicted in Fig. 2. The parameters are the maximum, the minimum, the mean and the 50th and 90th percentiles. The percentile reflects a value below which a given percentage of observations fall. As we can observe, the channel magnitude response decreases as the frequency increases, which configures a well know behavior of PLC channels [37]. Also, the minimum attenuation is lower than 10 dB for the frequencies below 50 MHz and between 10 and 18 dB in the remaining frequencies. On the other hand, attenuation as high as 100 dB can be observed in some channel responses. The mean values of magnitude attenuation per frequency component is between 20 and 40 dB, and such values are very close to the 50th percentile profile.

The empirical cumulative distribution function (CDF) of the magnitude responses for Band A, Band B and Band C, considering all samples of all estimated CFRs, are shown in Fig. 3. As we can note,

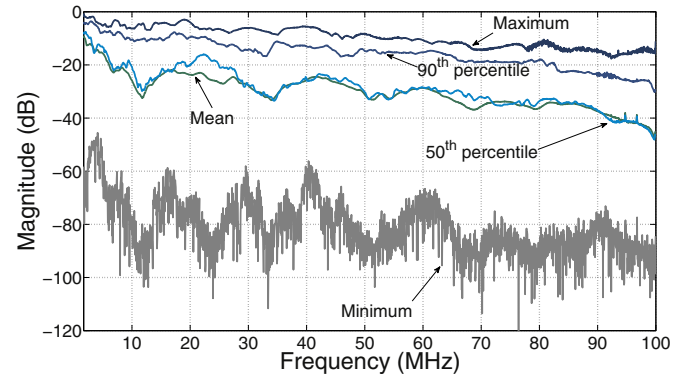


Fig. 2. General characterization of the measured in-home PLC channel magnitude response.

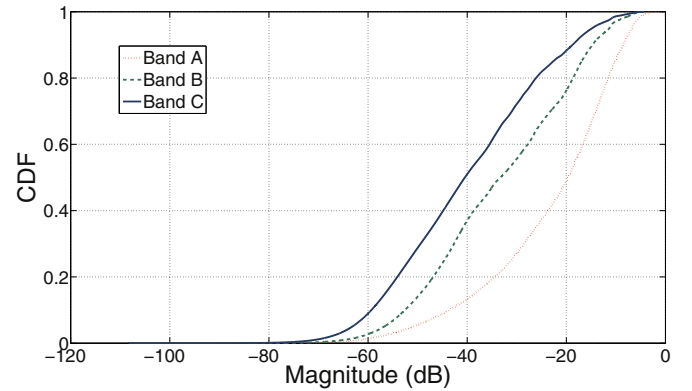


Fig. 3. Cumulative distribution function of the estimated in-home PLC channel magnitude responses.

the distance between Band B and Band C curves are, approximately, 6 dB, for the probabilities values between 0.2 and 0.8. In the same interval of probabilities, the distances between the curves for Band A and Band B reach almost 15 dB. Also, higher attenuation are found in Band C than in Band A and Band B, what agrees with the theory of signal propagation through a non-ideal conductor (attenuation increase with frequency). For instance, the probabilities that the attenuation is lower than 20 dB are 0.5, 0.7 and 0.9, approximately, for Band A, Band B and Band C, respectively. Additionally, this plot confirms that the in-home PLC channels are frequency selective.

5.2. Average channel attenuation

The ACA results are summarized in Table 2. Considering the Band A, the obtained results can be compared to those ones presented in [19] for in-home PLC systems in US. While the maximum, mean and minimum ACA values reported to US residences were around 68, 48.9 and 19 dB, respectively, for the Brazilian case they were around 51, 23.3 and 9 dB, indicating much lower attenuation levels in the Brazilian residences. From the authors point of view, the main reason for that distinct behavior is that the sizes of typical apartments and residences in Brazil are smaller than in US (see Table II in [38]). As a result, distances for data communication as well as the number of branches in US residences tend to be higher than in Brazilian residences considered in this work.

From the results presented in [18], for in-home PLC channels measured in Spain, the maximum magnitude values are similar to those ones measured in US [19], whereas the minimum values are close to the Brazilian values. In average, the Spanish ACA values are approximately 9 dB lower than the US ones but almost 20 dB higher than what was measured in Brazil. In other words, it means

Table 2
PLC channel average channel attenuation for Band A, Band B and Band C.

Average channel attenuation (dB)	Band A			Band B		Band C	
	Brazil	US	Spain	Brazil	Brazil	Italy	
	Maximum	51.09	68.12	≈70	52.62	55.27	57
Minimum	9.14	19.7	≈10	9.98	13.56	7.6	
Mean	23.28	48.9	≈30	25.24	30.21	35	
Standard Deviation	8.61	9.3	–	8.28	9.19	–	
50th percentile	22.77	49.2	–	25.67	30.82	–	
90th percentile	34.69	67.9	–	33.76	39.65	–	

Table 3
RMS-DS for the measured in-home PLC channels in Band A, Band B and Band C.

RMS-DS (μs)	Band A		Band B		Band C	
	Brazil	US	Brazil	Brazil	France	
	Maximum	0.49	1.81	0.47	0.46	1.04
Minimum	0.04	0.09	0.03	0.03	0.03	
Mean	0.15	0.53	0.14	0.13	0.31	
Std	0.06	0.29	0.06	0.06	0.21	
50th percentile	0.14	0.47	0.13	0.13	–	
90th percentile	0.23	1.75	0.21	0.20	0.60	

that Spanish ACA values are in between the ones from Brazil and US.

The results for Band B revealed that the mean ACA value expected in measured in-home Brazilian PLC channels is around 25 dB. Also, this value can reach a maximum of more than 52 dB. In the best scenario the maximum ACA value is less than 10 dB. Results for ACA in other countries for Band B are not found in the literature and the same occurs to other PLC channel features.

Considering the Band C, a minimum ACA of 13 dB and a maximum of 55 dB were observed. The mean ACA value for Band C is almost 8 dB and 5 dB higher than those ones for Band A and Band B, respectively. In Italy, the minimum ACA value is lower than in Brazil (7.6 dB) but the ACA can reach values up to 57 dB [14]. The mean ACA value observed in Italy is 35 dB, approximately, which is almost 5 dB higher than in Brazilian case.

5.3. Root mean squared delay spread

The obtained results for RMS-DS are summarized in Table 3. Regarding Band A, measured Brazilian in-home PLC channels show the smallest RMS-DS mean values (0.15 μs) in comparison to their US counterpart (0.53 μs) [19]. Also, the RMS-DS is above 0.47 μs in 50% of in-home PLC channels in US, against 0.14 μs for the same percentage in Brazil. For Band B the mean value observed for the RMS-DS is of 0.14 μs and for 90% of the observed cases this value is below 0.21 μs . Now considering Band C, a comparison with the results presented in [7] (French scenario) shows that the evaluated Brazilian in-home PLC channels present the smallest values for RMS-DS. While in France, the RMS-DS has mean value equal to 0.31 μs and can reach 0.60 μs in 90% of the cases, these values are 0.13 μs and 0.20 μs , respectively, in Brazil. From authors' point of view, the reasons for that are those appointed before for justifying the Brazilian ACA values.

5.4. RMS-DS versus ACA

A linear relationship between RMS-DS and ACA, which is usually expressed by (4), can be drawn as in Fig. 4. The parameters of (4) for the Brazilian in-home PLC channels are listed in Table 4. They are represented by the solid and straight lines in Fig. 4 for the three

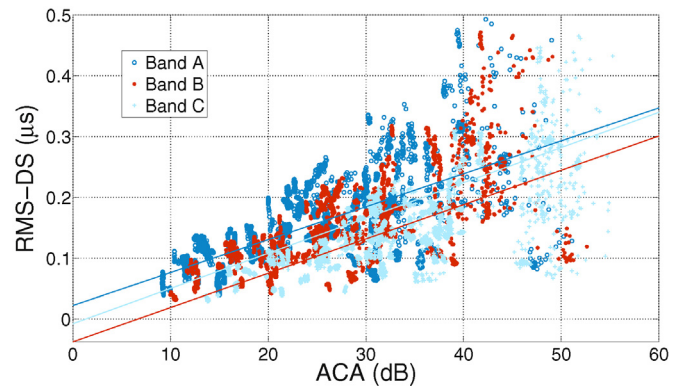


Fig. 4. Relationship between RMS-DS and ACA for the measured in-home PLC channels in Brazil.

Table 4
Parameters of (4) estimated for the measured PLC channels.

	α ($\mu\text{s}/\text{dB}$)	β (μs)
Band A	0.0054	0.0219
Band B	0.0058	−0.0079
Band C	0.0056	−0.0379

frequency bands considered in the current work. Surprisingly, the linear relationships between RMS-DS and ACA for Band A, Band B and Band C result in three almost parallel straight lines (α values are almost the same). Also, the dispersion around the trend is more accentuated for ACA values higher than 40 dB, approximately. Regarding Band A, a comparison among in-home PLC channels in US [13] and in Brazil shows that Brazilian counterparts present similar behavior to those channels from urban and suburban areas in US.

5.5. Coherence bandwidth

The obtained results for the CB are summarized in Table 5, considering the correlation level of 0.9.

Table 5
Coherence bandwidth estimated for the measured PLC channels.

Coherence bandwidth (kHz)	Band A		Band B	Band C	
	Brazil	Spain	Brazil	Brazil	France
	Maximum	2.78×10^3	$\approx 1.1 \times 10^3$	3.71×10^3	3.08×10^3
Minimum	97.66	–	146.48	97.66	43.5
Mean	644.29	–	720.55	780.27	310.1
Standard deviation	387.70	–	488.65	528.63	330.03
50th percentile	537.11	≈ 200	585.94	585.94	–
90th percentile	1.12×10^3	≈ 480	1.22×10^3	1.61×10^3	714.5

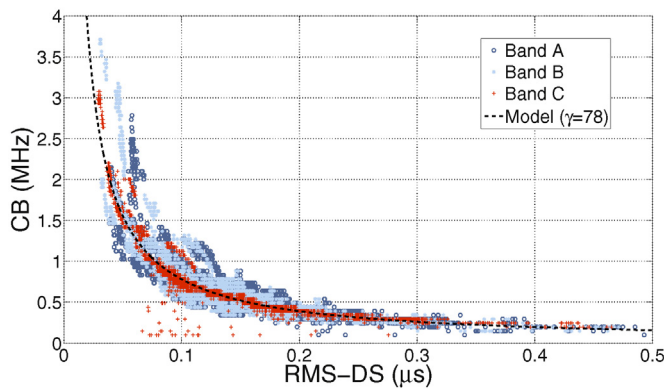


Fig. 5. Relationship between the coherence bandwidth and the RMS-DS for the in-home PLC channels in Brazil.

Comparing CB value with its Spanish [17] (for Band A) and French [7] (for Band C) counterparts, we notice a wider CB for Brazilian in-home PLC channels. Thus, measured in-home PLC channels in Brazil are flatter than in these countries. In fact, the maximum CB value observed in the considered places in Brazil is approximately 2.5 and 1.6 times its Spanish and French counterparts, respectively. In addition, while in 50% of measured Brazilian in-home PLC channels the CB is above 537 kHz, only about 10% of the Spanish in-home PLC channels present a CB above this value (see Fig. 4b in [17]).

For Band B, the mean value for CB is lower than those observed for Band A and higher than those observed for Band C. Also, while in 90% of the observed cases CB is below 1.12 MHz and 1.22 MHz for Band A and Band B, respectively, this value is below 1.61 MHz for Band A.

The CB values for the correlation levels of 0.5 and 0.7 can be accessed in A, through Tables A9 and A10, respectively.

5.6. CB versus RMS-DS

Fig. 5 shows the inverse relationship between RMS-DS and CB observed in Brazilian in-home PLC channels evaluated in this work, for all considered frequency bands. The best curve fitting for (7), which are represented by the dotted lines in the plot (only for the Band C), is based on the minimum mean square error (MMSE) criterion. The least-square curve fitting yield $\gamma = 77$, $\gamma = 77$ and $\gamma = 78$ for Band A, Band B and Band C, respectively. For comparison purposes, $\gamma = 55$ was attained with French in-home PLC channels [7], while $\gamma = 57$ was obtained with Italian PLC channels [14], both for Band C.

5.7. Temporal variation analysis

In this analysis only 196 PLC channels (pair of outlets) that rendered more than 644 consecutive estimates of frequency response were taken into account. This is because some channel estimates, as those affected by impulsive noise, were removed from the data set.

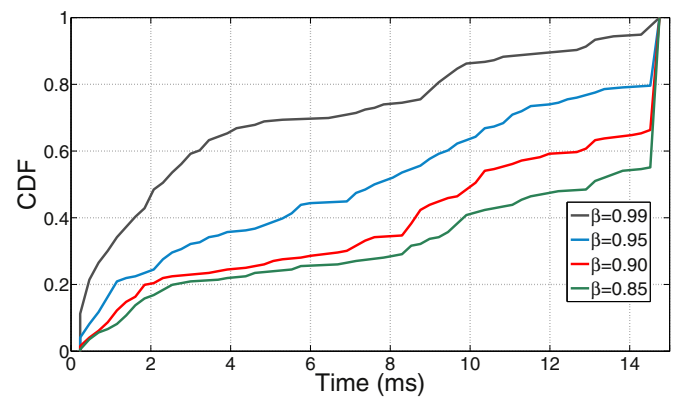


Fig. 6. CDF of the CIR coherence time for Band C.

Table 6

Maximum and minimal variation of each channel feature among the estimates of the same channel.

	Maximum	Minimum
ACA	1.87 dB	0.22 dB
CB	830.08 kHz	48.83 kHz
RMS-DS	374.8 ms	3.8 ms

Each of these considered PLC channels was evaluated in a period of time that corresponds to almost 90% the duration of one cycle of the mains signal, since the mains frequency is of 60 Hz in Brazil and each channel estimate occurs in approximately 23 μ s.

The correlation among consecutive CIR is performed in order to calculate the coherence time of PLC channels, as discussed in [35]. The resulting CDF of the CT for Band C is shown in Fig. 6, in which correlation levels of 0.85, 0.90, 0.95 and 0.99 are adopted. The CT 50% percentile is about 2 ms for $\beta = 0.99$; 7.4 ms for $\beta = 0.95$; 10 ms for $\beta = 0.90$ and more than 13 ms for $\beta = 0.85$. The results related to Band A and Band B were suppressed because the probability of a CT be lower than a given value is almost the same for all analyzed frequency bands.

Time variation of ACA, CB (only for the correlation level of 0.9) and RMS-DS were evaluated using Algorithm 1 and, for sake of simplicity, only Band C was considered. The maximum and minimum variation of the analyzed channel features observed among the consecutive estimates related to the same measured channel is presented in Table 6. Worth noting the low variation observed for ACA between consecutive estimates of the same channel, that is below 2 dB.

Basically, Algorithm 1 encounter periods of time in which the temporal difference between two estimates of a certain channel feature (ACA, CB or RMS-DS) reaches a given threshold ($\epsilon \in \mathbb{R} | \epsilon > 0$). The sequence $\{M_i[n]\}$, with $n = 1, 2, \dots, m$, represents consecutive estimates of ACA, CB or RMS-DS, related to the i th PLC channel (pair of outlets), where $m = 644$. The thresholds are listed in Table 7. They were chosen based on Table 6. The CDFs of the time variation

Table 7
Set of chosen threshold (ϵ) used in **Algorithm 1** in order to evaluate time variation of ACA, CB and RMS-DS.

Scenarios	A	B
ACA (dB)	0.3	0.6
CB (kHz)	30	60
RMS-DS (ms)	10	60

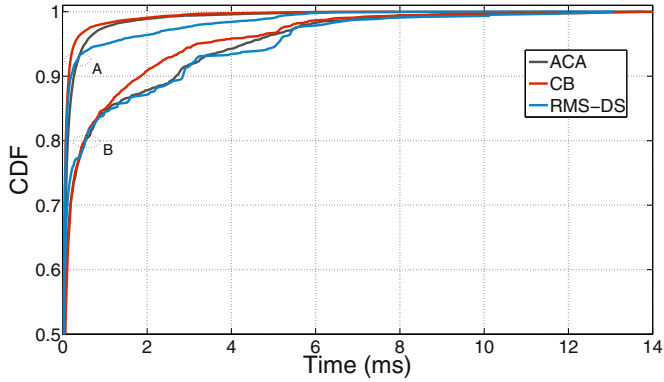


Fig. 7. CDF of PLC channel feature time variation.

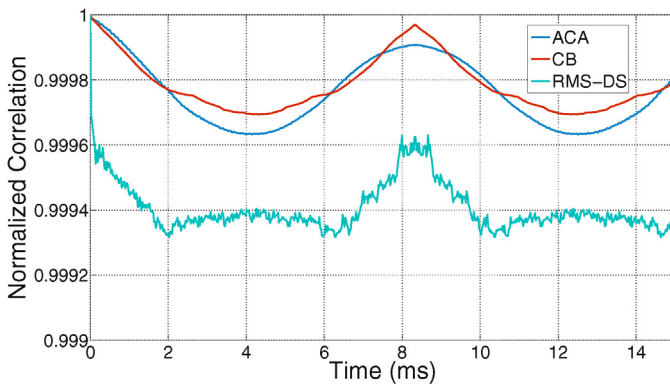


Fig. 8. Correlation between channel parameters and mains signal.

of ACA, CB and RMS-DS are shown in **Fig. 7**. As can be seen, ACA can take less than 2.2 ms to vary 0.3 dB, and less than 7.6 ms to vary 0.6 dB in 99% of cases. Regarding CB, we see that it can vary 30 kHz in a time interval less than 2 ms and 60 kHz in up to 6.8 ms in 99% of the observed estimates. Moreover, **Fig. 7** shows that RMS-DS can vary 0.01 μ s in up to 5 ms, and take about 7.7 ms to vary 0.06 μ s, in 99% of cases.

Algorithm 1. Algorithm used to evaluate time variation of channel feature.

```

Data:  $\{M_i[n]\}$ 
Result:  $\{E_i[n]\}$ 
Initialization:  $n = 0, k, l = 1;$ 
while  $l \neq m - l$  do
  if  $|M_i[k] - M_i[l]| > \epsilon$  then
     $n = n + 1;$ 
     $E_i[n] = l - k;$ 
     $k = l;$ 
  end
   $l = l + 1;$ 
end

```

Let now **Fig. 8**, in which is shown the temporal relationship between channel parameters and mains signal amplitude. Each

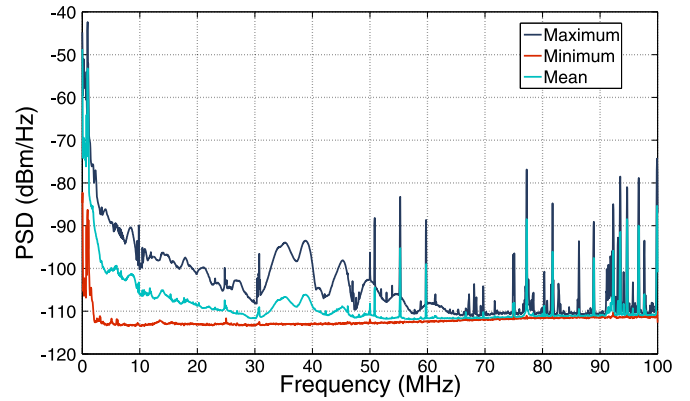


Fig. 9. Estimated noise PSD in the measured in-home PLC channel.

curve is the result of the correlation between consecutive estimates of a channel parameter (ACA, CB and RMS-DS) related to one measured PLC channel, tacked as an example. We see that correlation curves present periodically time varying behavior in which their peaks are periodic with a period of, approximately, a half of the mains signal period (≈ 8.33 ms). Moreover, these curves reinforces that in-home PLC channel is cyclically time varying channel. On the other hand, based on the values of these correlation curves, it is clear that ACA, CB and RMS-DS does not change significantly within the time duration of one mains cycle. Again, only Band C was considered in this analysis.

5.8. Power spectral density of the additive noise

In in-home PLC channels, the noise behaves as a sum of several kinds of disturbances. Indeed, the noise in power lines are classified in three distinct groups [39]: background noise, with high energy in low frequencies; narrowband noise, in which occurs in a portion of the frequency spectrum in some instants of time and are generally due to broadcast signals; and impulsive noise, with short duration and high energy, that can be periodically synchronous or asynchronous in relation to the mains signal, produced for some kind of appliances, or asynchronous impulses due to load switching or some fault.

The measured additive noise is analyzed by means of PSD, and no significant impulsive noise event was observed in the time domain. The PSD was estimated by means of the Welch method described in [40] and is showed in **Fig. 9**. The higher peaks in the graphic, mainly above 50 MHz, are recognized as narrowband noise components. These components cover broadcast signals, such as FM and amateur radio, that are inducted into power lines. The decreasing PSD value with frequency is similar to what has been observed in previous works [41]. The analysis of several samples of measured additive noise shows that the PSD values range from -112 dBm/Hz, approximately, up to almost -42 dBm/Hz. The high PSD value is associated with the low-frequency components. The maximum-, mean- and minimum-value PSD curves reveal the presence of several primary users (each one associated with a narrowband signal).

5.9. Achievable data rate

The results for achievable data rates are approximated because the use of (9) leads to an overestimation of their values. This is because the data transmission is considered over all frequency band. In fact, in real transmission some frequency bands must be avoided according to the imposed regulation rules, which depends on each country.

The maximum, mean and minimum data rate estimates of the measured Brazilian in-home PLC channels are shown in **Fig. 10**.

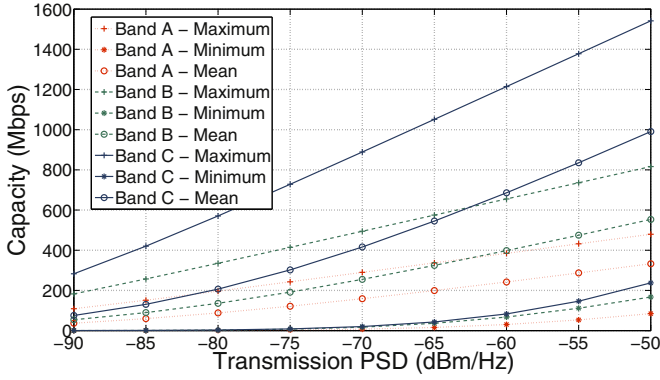


Fig. 10. Achievable data rate of the measured in-home PLC channels.

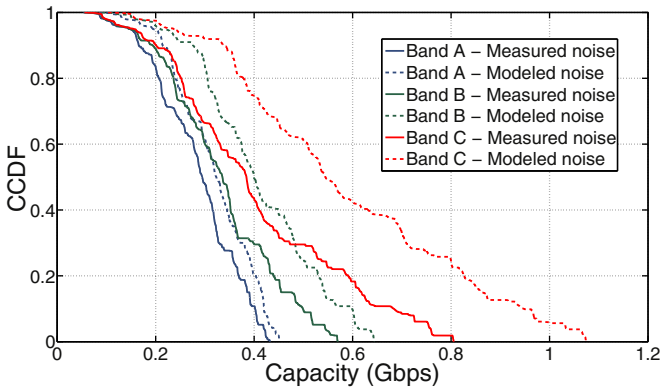


Fig. 11. Complementary CDF of achievable data rate using the measured and modeled noise.

These curves were obtained by considering Band A, Band B and Band C, where the PSD of the transmitted signal ranges from -90 up to -50 dBm/Hz and estimates of noise PSD are based on measured additive noise. The following observations can be drawn looking at these curves: (i) the mean achievable data rates are closer to the maximum ones than to the minimum; (ii) considerable difference in terms of achievable data rate can be observed when comparing the results for the three chosen frequency bands.

The complementary CDF (CCDF) of achievable data rate is shown in Fig. 11. These curves took into account the use of measured additive noise and the colored noise given by [42]

$$S_N(f) = 10 \log_{10} \left(\frac{1}{f^2} + 10^{-15.5} \right) \text{ [dBm/Hz]}. \quad (10)$$

In order to comply with the electric field emission regulation applied to PLC systems [43], the curves were obtained when the PSD of the transmitted signal is -55 dBm/Hz in the frequency band that corresponds to Band A and -80 dBm/Hz in the remaining frequencies up to 100 MHz. Comparing results when using the measured additive noise and colored additive noise model, the achievable data rate evaluated applying the model for the additive noise seems to be very appropriate for the Band A and very optimistic for the Band B and Band C and, as a consequence, it may not be useful to represent the PSD of additive noise in Brazilian premises. Overall, achievable data rate of measured Brazilian in-home PLC channels is higher than in Italy (see Figure 11 and Table IX in [14]), for the same PSD model given by (10).

5.10. Access impedance

The PLC access impedance was measured considering the frequency band ranging from 2 MHz up to 100 MHz. The results for

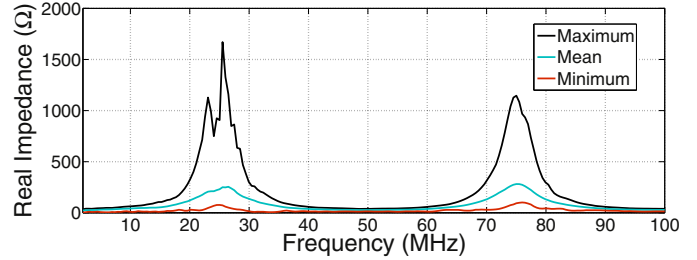


Fig. 12. Real access impedance.

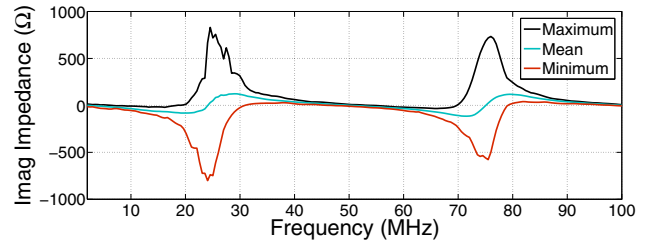


Fig. 13. Imaginary access impedance.

Table 8
PLC channel access impedance.

	Real impedance (Ω)	Imaginary impedance (Ω)
Maximum	1.67×10^3	829.73
Minimum	2.18	-801.23
Mean	81.52	5.3
Standard deviation	97.11	91.37
50th percentile	46.28	3.44
90th percentile	173.20	96.89

real (resistance) and imaginary (reactance) impedances for each considered frequency are depicted in Figs. 12 and 13, respectively. As can be observed, the access impedance presented higher values of resistance and reactance in the frequency bands between 15 and 35 MHz and between 65 and 85 MHz. In the remainder frequencies the access impedance variation between measurements was more discrete.

Some statistical results for PLC access impedance are summarized in Table 8. As can be observed, the resistance can vary in a large scale ranging from 2.18Ω up to $1.67 \text{ k}\Omega$. On the other hand, in 90% of the measured cases the resistance was below 173.20Ω . The values for reactance range from -801.23 up to 829.73Ω with a mean value of 5.3Ω . Furthermore, the reactance values shows that measured access impedance of PLC channels can present inductive and capacitive characteristics.

6. Conclusions

This work presented and discussed several features of seven Brazilian in-home PLC channels, which are relevant for modeling and designing PLC systems. Also, the analysis for the frequency band regulated in Brazil for PLC systems operation (from 1.7 up to 50 MHz) constitute an important reference to development of PLC systems to operate in Brazilian in-home electric power grids. The features considered here included the average channel gain or attenuation, the coherence bandwidth, the root mean squared delay spread, the coherence time, the achievable data rate and the noise profile.

The comparisons performed in this work reinforce the assumption that electric power grids in in-home facilities can have a strong disparate in different locations. From this contribution, some

important information related to measured Brazilian in-home PLC channel can be highlighted:

- The mean values for the channel magnitude function are between -10 and -40 dB for the chosen frequency bands.
- The estimated channel attenuation presents values below those reported in US and Europe (France, Spain and Italy).
- The estimated root mean squared delay spread presents values below those reported in US and Europe (France and Spain).
- The coherence bandwidth values are higher than those in Europe (France and Spain).
- A linear relationship between average channel attenuation and root mean squared delay spread (approximately co-linear for all chosen frequency bands) and an inverse relationship between coherence bandwidth and root mean squared delay spread are confirmed.
- The coherence time is above of $950 \mu\text{s}$ in 90% of the cases, considering a correlation level of 0.90, independent of the chosen frequency band. This result is greater than the coherence time of in-home PLC channel reported in the literature, which is of $600 \mu\text{s}$;
- The ACA presented very short variation between consecutive estimates of the same channel, while CB and RMS-DS can vary up to 830 kHz and 374 ms, respectively;
- The measured PLC channels presented a cyclically time varying behavior, with a period equal to a half of the mains signal cycle duration;
- The data rate can achieve maximum values of 0.42, 0.76 and 1.38 Gbps, approximately, for the frequency band from 1.7 up to 30 MHz, from 1.7 up to 50 MHz and from 1.7 up to 100 MHz, respectively, when the PSD of the transmission signal is equal to -55 dBm/Hz.
- The access impedance can vary its real part in a large scale ranging from 2.18Ω up to $1.67 \text{ k}\Omega$. The values for imaginary part revealed that PLC access impedance can have inductive and capacitive characteristics.

Overall, based on the results, we can point out that measured Brazilian in-home PLC channels seem to be more suitable for data communication purposes than the PLC channels in countries such as US, France and Spain. This behavior can be probably associated to the shorter channel length of the Brazilian residences evaluated in this contribution in comparison with those channels measured in other countries.

Acknowledgements

The authors would like to thank IFSEMG, FINEP, FAPEMIG, CNPq, CAPES, P&D ANEEL, CEMIG, INERGE and Smarti9 for their financial supports. We are very grateful to Dr. Stefano Galli for having nice discussions that help us to finish this work.

Appendix A. Coherence bandwidth results.

Tables A9 and A10 refer to the results for coherence bandwidth related to correlation levels of 0.5 and 0.7, respectively.

Table A9

Coherence bandwidth estimated for the measured PLC channels for correlation level of 0.5.

Coherence bandwidth (kHz)			
	Band A	Band B	Band C
Maximum	28.27×10^3	48.29×10^3	95.22×10^3
Minimum	341.79	390.62	439.45
Mean	4.19×10^3	3.99×10^3	7.99×10^3

Table A9 (Continued)

Coherence bandwidth (kHz)			
	Band A	Band B	Band C
Standard deviation	4.88×10^3	4.02×10^3	15.21×10^3
50th percentile	2.78×10^3	2.73×10^3	2.93×10^3
90th percentile	7.18×10^3	7.18×10^3	12.94×10^3

Table A10

Coherence bandwidth estimated for the measured PLC channels for correlation level of 0.7.

Coherence bandwidth (kHz)			
	Band A	Band B	Band C
Maximum	7.47×10^3	10.64×10^3	38.04×10^3
Minimum	195.31	244.14	97.66
Mean	1.77×10^3	1.90×10^3	2.67×10^3
Standard deviation	1.21×10^3	1.42×10^3	4.49×10^3
50th percentile	1.37×10^3	1.42×10^3	1.66×10^3
90th percentile	3.27×10^3	3.71×10^3	3.61×10^3

References

- [1] M.-Y. Zhai, Transmission characteristics of low-voltage distribution networks in China under the smart grids environment, *IEEE Trans. Power Deliv.* 26 (1) (2011) 173–180.
- [2] A.G. Lazaropoulos, P.G. Cottis, Transmission characteristics of overhead medium-voltage power-line communication channels, *IEEE Trans. Power Deliv.* 24 (3) (2009) 1164–1173.
- [3] A. Cataliotti, A. Daidone, G. Tine, A medium-voltage cables model for power-line communication, *IEEE Trans. Power Deliv.* 24 (1) (2009) 129–135, <http://dx.doi.org/10.1109/TPWRD.2008.2002664>.
- [4] M. Zajc, N. Suljanovic, A. Mujcic, J.F. Tasic, High voltage power line constraints for high speed communications, in: *Proc. Mediterranean Electrotechnical Conference*, vol. 1, 2004, pp. 285–288.
- [5] R. Aquilue, M. Ribo, J.R. Regue, J.L. Pijoan, G. Sanchez, Scattering parameters-based channel characterization and modeling for underground medium-voltage power-line communications, *IEEE Trans. Power Deliv.* 24 (3) (2009) 1122–1131.
- [6] P. Amirshahi, M. Kavehrad, High-frequency characteristics of overhead multiconductor power lines for broadband communications, *IEEE J. Sel. Areas Commun.* 24 (7) (2006) 1292–1303, <http://dx.doi.org/10.1109/JSA.2006.874399>.
- [7] M. Tlich, A. Zeddou, F. Moulin, F. Gauthier, Indoor power-line communications channel characterization up to 100 MHz – Part II: time-frequency analysis, *IEEE Trans. Power Deliv.* 23 (3) (2008) 1402–1409.
- [8] A.B. Vallejo-Mora, J.J. Sanchez-Martinez, F.J. Canete, J.A. Cortes, L. Diez, Analysis of in-vehicle power line channel response, *IEEE Latin Am. Trans.* 9 (4) (2011) 445–450.
- [9] S. Barmada, L. Bellanti, M. Raugi, M. Tucci, Analysis of power-line communication channels in ships, *IEEE Trans. Veh. Technol.* 59 (7) (2010) 3161–3170.
- [10] C.H. Jones, Communications over aircraft power lines, in: *Proc. IEEE International Symposium on Power Line Communications and Its Applications*, 2006, pp. 149–154.
- [11] H. Gassara, F. Rouissi, A. Ghazel, Statistical characterization of the indoor low-voltage narrowband power line communication channel, *IEEE Trans. Electromagn. Compat.* 56 (1) (2014) 123–131.
- [12] A.I. Chrysochos, T.A. Papadopoulos, A. ElSamadouny, G.K. Papagiannis, N. Al-Dhahir, Optimized mimo-ofdm design for narrowband-plc applications in medium-voltage smart distribution grids, *Electr. Power Syst. Res.* 140 (2016) 253–262.
- [13] S. Galli, A novel approach to the statistical modeling of wireline channels, *IEEE Trans. Commun.* 59 (5) (2011) 1332–1345.
- [14] A.M. Tonello, F. Versolatto, A. Pittolo, In-home power line communication channel: statistical characterization, *IEEE Trans. Commun.* 62 (6) (2014) 2096–2106.
- [15] F. Versolatto, A.M. Tonello, PLC channel characterization up to 300 MHz: frequency response and line impedance, in: *Proc. IEEE Global Communications Conference*, 2012, pp. 3525–3530.
- [16] F.J. Canete, L. Diez, J.A. Cortes, J.T. Entrambasaguas, Broadband modelling of indoor power-line channels, *IEEE Trans. Consum. Electron.* 48 (1) (2002) 175–183.
- [17] F.J. Canete, J.A. Cortes, L. Diez, J.T. Entrambasaguas, A channel model proposal for indoor power line communications, *IEEE Commun. Mag.* 49 (12) (2011) 166–174.
- [18] J.A. Cortes, F.J. Canete, L. Diez, J.L.G. Moreno, On the statistical properties of indoor power line channels: measurements and models, in: *Proc. IEEE International Symposium on Power Line Communications and Its Applications*, 2011, pp. 271–276.

- [19] S. Galli, A simplified model for the indoor power line channel, in: Proc. IEEE International Symposium on Power Line Communications and Its Applications, 2009, pp. 13–19.
- [20] A.M. Tonello, F. Versolatto, B. Béjar, S. Zazo, A fitting algorithm for random modeling the PLC channel, IEEE Trans. Power Deliv. 27 (3) (2012) 1477–1484.
- [21] F.J. Canete, J.A. Cortes, L. Diez, J.T. Entrambasaguas, Analysis of the cyclic short-term variation of indoor power line channels, IEEE J. Sel. Areas Commun. 24 (7) (2006) 1327–1338.
- [22] F. Gianaroli, F. Pancaldi, G.M. Vitetta, On the use of Zadeh's series expansion for modeling and estimation of indoor powerline channels, IEEE Trans. Commun. 62 (7) (2014) 2558–2568.
- [23] C.J. Kikkert, S. Zhu, Measurement of powerlines and devices using an inductive shunt on-line impedance analyzer, in: Proc. IEEE International Symposium on Power Line Communications and Its Applications, 2015, pp. 41–46.
- [24] J. Valencia, T.R. Oliveira, F.J.A. Andrade, M.V. Ribeiro, Statistical analysis of Brazilian in-home PLC channels: first results, in: Proc. IEEE International Symposium on Power Line Communications and Its Applications, 2014, pp. 127–131.
- [25] ANATEL, Brazilian resolution for PLC, 2009 <http://legislacao.anatel.gov.br/resolucoes/2009/101-resolucao-527>.
- [26] S. Galli, T. Banwell, A novel approach to the modeling of the indoor power line channel—part II: transfer function and its properties, IEEE Trans. Power Deliv. 20 (3) (2005) 1869–1878.
- [27] Gage, Arbitrary waveform generator data-sheet. <http://www.gage-applied.com/arbitrary-waveform-generators/GaGe-AWG-CG4300-4302-PCI-Data-Sheet.pdf> (accessed 18.04.17).
- [28] Gage, Data digitizer data-sheet. <http://www.gage-applied.com/digitizers/GaGe-Digitizer-RazorExpressCS-PCle-Data-Sheet.pdf> (accessed 18.04.17).
- [29] L.G. da Silva Costa, A.C.M. de Queiroz, B. Adebisi, V.L.R. da Costa, M.V. Ribeiro, Coupling for power line communications: a survey, J. Commun. Inf. Syst. 32 (1) (2017).
- [30] M.V. Ribeiro, G.R. Colen, F.V.P. de Campos, Z. Quan, H.V. Poor, Clustered-orthogonal frequency division multiplexing for power line communication: when is it beneficial? IET Commun. 8 (13) (2014) 2336–2347.
- [31] T.R. Oliveira, C.A.G. Marques, W.A. Finamore, S.L. Netto, M.V. Ribeiro, A methodology for estimating frequency responses of electric power grids, J. Control Autom. Electr. Syst. (online published) 25 (6) (2014) 720–731.
- [32] F.M. Gardner, Interpolation in digital modems. I. Fundamentals, IEEE Trans. Commun. 41 (3) (1993) 501–507.
- [33] T. Keller, L. Hanzo, Orthogonal frequency division multiplex synchronization techniques for wireless local area networks, in: Proc. IEEE International Symposium on Personal, Indoor and Mobile Radio Communications, vol. 3, 1996, pp. 963–967.
- [34] D.F. Cardoso, F.D. Backx, R. Sampaio-Neto, Improved pilot-aided channel estimation in zero padded MC-CDMA systems, in: Proc. International Symposium on Wireless Pervasive Computing, 2009, pp. 1–5.
- [35] A.A.M. Picorone, R. Sampaio-Neto, M.V. Ribeiro, Coherence time and sparsity of Brazilian outdoor PLC channels: a preliminary analysis, in: Proc. IEEE International Symposium on Power Line Communications and Its Applications, Glasgow, United Kingdom, 2014, pp. 1–5.
- [36] T.M. Cover, J.A. Thomas, Elements of Information Theory, John Wiley & Sons, 2006.
- [37] H.C. Ferreira, L. Lampe, J. Newbury, T.G. Swart, Power Line Communications: Theory and Applications for Narrowband and Broadband Communications over Power Lines, 1st Ed., WILEY, 2010.
- [38] B. O'Mahony, Field testing of high-speed power line communications in North American homes, in: Proc. IEEE International Symposium on Power Line Communications and Its Applications, 2006, pp. 155–159.
- [39] M. Zimmermann, K. Dostert, Analysis and modeling of impulsive noise in broad-band powerline communications, IEEE Trans. Electromag. Compat. 44 (1) (2002) 249–258, <http://dx.doi.org/10.1109/15.990732>.
- [40] P. Welch, The use of fast Fourier transform for the estimation of power spectra: a method based on time averaging over short, modified periodograms, IEEE Trans. Audio Electroacoust. 15 (2) (1967) 70–73.
- [41] M. Zimmermann, K. Dostert, Analysis and modeling of impulsive noise in broad-band powerline communications, IEEE Trans. Electromag. Compat. 44 (1) (2002) 249–258.
- [42] R. Hashmat, P. Pagani, A. Zeddam, T. Chonavel, MIMO communications for inhome PLC networks: measurements and results up to 100 MHz, in: Proc. IEEE International Symposium on Power Line Communications and Its Applications, 2010, pp. 120–124.
- [43] B. Praho, M. Tlich, P. Pagani, A. Zeddam, F. Nouvel, Cognitive detection method of radio frequencies on power line networks, in: Proc. IEEE International Symposium on Power Line Communications and Its Applications, 2010, pp. 225–230.